# Oxidative stress-inducible truncated serine/arginine-rich splicing factor 3 regulates interleukin-8 production in human colon cancer cells

Shizuka Kano*, Kensei Nishida*, Hiroyuki Kurebe, Chihiro Nishiyama, Kentaro Kita, Yoko Akaike, Keisuke Kajita, Ken Kurokawa, Kiyoshi Masuda, Yuki Kuwano, Toshihito Tanahashi, and Kazuhito Rokutan

*Department of Stress Science, Institute of Health Biosciences, The University of Tokushima Graduate School, Tokushima 770-8503, Japan*

*These authors contributed equally to this study.

*Running Title:* Truncated SRSF3 regulates IL-8 production

Corresponding author: Kazuhito Rokutan, MD, PhD

Department of Stress Science, Institute of Health Biosciences, The University of Tokushima Graduate School, 3-18-15 Kuramoto-cho, Tokushima 770-8503, Japan

E-mail: rokutan@tokushima-u.ac.jp

Phone: +81-88-633-9007 Fax: +81-88-633-9008

**ABSTRACT**

**Serine/arginine-rich splicing factor 3 (SRSF3) is a member of the SR protein family and plays wide-ranging roles in gene expression. The human *SRSF3* gene generates two alternative splice transcripts, a major mRNA isoform (*SRSF3-FL*) encoding functional full-length protein and a premature termination codon (PTC)-containing isoform (*SRSF3-PTC*). The latter is degraded through nonsense-mediated mRNA decay (NMD). Treatment of a human colon cancer cell line (HCT116) with 100 μM sodium arsenite increased *SRSF3-PTC* mRNA levels without changing *SRSF3-FL* mRNA levels. A chemiluminescence-based NMD reporter assay system demonstrated that arsenite treatment inhibited NMD activity and increased *SRSF3-PTC* mRNA levels in the cytoplasm, facilitating translation of a truncated SRSF3 protein (SRSF3-TR) from *SRSF3-PTC* mRNA. SRSF3-TR lacked two-thirds of Arg/Ser-rich (RS) domain whose phosphorylation state is known to be crucial for subcellular distribution. SRSF3-FL was localized in the nucleus, while overexpressed SRSF3-TR was diffusely distributed in the cytoplasm and the nucleus. A part of SRSF3-TR was also associated with stress granules in the cytoplasm. Interestingly, treatment of HCT116 cells with a small interference RNA specifically targeting *SRSF3-PTC* mRNA significantly attenuated arsenite-stimulated induction of c-JUN protein, its binding activity to the AP-1 binding site (-126 to 120 bp) in the *interleukin (IL)-8* gene promoter, and AP-1 promoter activity, resulting in significant reduction of arsenite-stimulated IL-8 production. Our results suggest that SRSF3-TR may function as a positive regulator of oxidative stress-initiated inflammatory responses in colon cancer cells.**

**Keywords: *SRSF3* gene; oxidative stress; alternative splicing; nonsense-mediated mRNA decay; IL-8**

A serine/arginine-rich splicing factor 3 (SRSF3) (also known as SRp20) is a member of the SR protein family which comprises at least 12 evolutionarily conserved and structurally related RNA-binding proteins (SRSF1 to SRSF12) (24). Like other SR proteins, SRSF3 binds *cis*-acting RNA elements through an N-terminal RNA recognition motif (RRM), and a C-terminal region enriched in Arg–Ser dipeptides (RS domain) mediates interactions with other proteins for regulation of both constitutive and alternative splicing of pre-mRNA (7). Recently, it has been shown that SR protein family, including SRSF3, participates in many cellular processes including transcriptional elongation (22), mRNA transport (32), translation (31), and cell cycle regulation (16). In addition, a short hairpin RNA-based screen of splicing regulators has uncovered a novel function of SRSF3 as a negative regulator of interleukin (IL)-1β (28). Moreover, SRSF3 is overexpressed in human ovarian cancer, and its knockdown results in apoptosis of ovarian cancer cells (10). These findings suggest that SRSF3 contributes to biological networks for cell fate.

The human *SRSF3* gene is composed of 7 exons and 8 introns, and generates two mRNA isoforms through alternative splicing. *SRSF3* exon 4 contains multiple premature stop codons (PTCs); therefore, a major *SRSF3* mRNA isoform, which encodes a functional full-length SRSF3 protein (SRSF3-FL), excludes this exon 4. Alternative splicing of *SRSF3* pre-mRNA produces another mRNA isoform consisting of entire 7 exons. This PTC-containing *SRSF3* isoform (*SRSF3-PTC*) should be degraded through nonsense-mediated mRNA decay (NMD), a surveillance mechanism that decomposes PTC-containing mRNAs. However, this isoform is considered to contribute auto-regulation of its own mRNA expression in a cell cycle specific manner (12). At the same time, it was reported that *SRSF3-PTC* mRNA was translatable into a truncated SRSF3 protein (SRSF3-TR) partially lacking RS domain in the murine B-cell lymphoma K46 cells (12). However, the biological function of SRSF3-TR remains to be elucidated.

In this study, we showed that significant amounts of SRSF3-TR were translated from

*SRSF3-PTC* mRNA in colon cancer cells exposed to an oxidant (sodium arsenite). Moreover, we suggest that SRSF-TR may function as a positive regulator of oxidative stress-stimulated production of IL-8 through regulating c-JUN expression. The present study may provide a new insight into the biological function of PTC-containing mRNAs of the SR protein family genes.

## MATERIALS AND METHODS

*Cell culture and subcellular fractionation.* HCT 116 cells were cultured in McCoy's 5A medium (Gibco, Grand Island, NY) supplemented with 5% (vol/vol) heat-inactivated fetal bovine serum and antibiotics at 37°C in 5% $CO_2$. After HCT116 cells were incubated in lysis buffer (10 mM Tris-HCl, pH 7.4; 100 mM NaCl; 2.5 mM $MgCl_2$; 40 μg/ml digitonin) for 10 min, lysates were centrifuged at 2,060 *g* for 8 min at 4°C, and supernatants were collected as cytosolic extracts. The remaining pellets were washed twice with the lysis buffer and further lysed with RIPA buffer (10 mM Tris-HCl, pH 7.4; 150 mM NaCl; 1 mM EDTA; 1 mM DTT; 0.1% SDS; 1% NP-40) containing a protease and phosphatase inhibitor cocktail (Sigma-Aldrich, St. Louis, MO). After centrifugation at 21,000 *g* for 10 min at 4°C, supernatants were collected as nuclear extracts. Cells lysed with RIPA buffer were used as whole-cell extracts (18).

*Plasmid construction.* A cDNA library was prepared from HCT116 cells, and the human *SRSF3* mRNAs (Ensembl Transcript ID: ENST00000373715 (*SRSF3-FL*) and ENST00000477442 (*SRSF3-PTC*)) were amplified by PCR using a primer set: 5'-AAAAAAGGATCCATGCATCGTGATTCCTGTCCATTG-3' (forward; BamHI site is underlined) and 5'-AAAAAAGATATCCTATTTCCTTTCATTTGACCTAGA-3' (reverse;

EcoRV site is underlined). The amplified products were separated using a gel extraction kit (Qiagen, Hilden, Germany) and cloned into the mammalian expression vector pCMV-3Tag (Stratagene, La Jolla, CA). FLAG was appended to the $NH_2$ termini of SRSF3. All constructs were confirmed to have the expected sequence by DNA sequencing. These plasmids were transfected using FuGENE HD (Promega, Madison, WI) according to the manufacturer's instructions.

*Small interference RNAs (siRNAs)*. We used a small interference (si) RNA (Stealth RNAi, Invitrogen, Carlsbad, CA) targeting exon 4; 5'-TCAACTAGCCCTTTCAGCGTCATGT-3' (*SRSF3-PTC* siRNA) to selectively silence *SRSF3-PTC* mRNA and SRSF3-TR protein. To inhibit NMD system, an siRNA targeting *up-frameshift-1* (*UPF1;* Invitrogen); 5'-UAAACUCGUCACCAAGGUAACU-3' was introduced to HCT116 cells. The Stealth RNAi negative control (Invitrogen) was used as a control siRNA. HCT116 cells were transfected with 10 nM of one of these siRNAs using Lipofectamine RNAiMAX (Invitrogen).

*Quantitative real-time reverse transcription-PCR (qPCR).* Total RNAs were extracted from HCT116 cells using an RNAiso plus (Takara, Otsu, Japan). One microgram of isolated RNA was reverse-transcribed using ReverTra Ace reverse transcriptase (TOYOBO, Osaka, Japan). *SRSF3-FL, SRSF3-PTC, IL-8, IL-1β, IL-6, IFN-γ, and TNF-α* mRNA levels were measured using SYBR green master mix and the 7500 real-time system (Applied Biosystems, Foster City, CA). *Glyceraldehyde 3-phosphate dehydrogenase* (*GAPDH*) mRNA and *18S* were measured as internal controls for normalization. Using the ΔΔCt method, the data are presented as the fold change in gene expression relative to controls measured in the untreated or control siRNA-treated cells. The sequences of primer sets used are shown in Table 1.

*Inhibition of NMD activity and chemiluminescence-based NMD assay*. To inhibit the

NMD system, HCT116 cells were treated with 50 or 100 μg/ml cycloheximide for 6 h or with 10 nM *UPF1* siRNA for 48 h. Plasmids containing pCI-neo β-globin-wt (WT), pCI-neo β-globin-NS39 (NS39), and pCI-neo-firefly were kindly provided by Dr. Kulozik and used for chemiluminescence-based NMD assay (3). Twenty-four hours after pretreatment of HCT116 cells with control or *SRSF-PTC* siRNA, they were co-transfected with pCI-neo-firefly and WT or NS39, and then incubated for another 24 h. These cells were left untreated or treated with 100 μM arsenite for the indicated times. Cell lysates were prepared, and renilla and firefly luciferase activities were measured with dual luciferase assay system (Promega) according to the manufacturer's protocol. The transfection efficacy was assessed by firefly luciferase activity.

*Measurement of IL-8 concentration in the culture medium*. After treatment of HCT116 cells with control or *SRSF3-PTC* siRNA for 24 h, they were exposed to 100 μM arsenite for the indicated times, and supernatants were collected. Cell debris were removed by centrifugation at 10,000 *g* for 5 min at 4°C, and the resultant supernatants were subjected to ELISA measurement of IL-8 using a commercially available ELISA kit (Biolegend, San Diego, CA) according to the protocols provided by the manufacturer.

*Western blotting*. Whole-cell lysates were prepared in RIPA buffer (10 mM Tris-HCl, pH 7.4; 150 mM NaCl; 1 mM EDTA; 1 mM DTT; 0.1% SDS; 1% NP-40) containing a protease and phosphatase inhibitor cocktail (Sigma-Aldrich). The extracted proteins were separated by SDS-PAGE and transferred to a polyvinylidene difluoride membrane (BioRad, Hercules, CA). After blocking with 5% non-fat dry milk, the membranes were incubated overnight at 4°C with a mouse monoclonal anti-SRSF3 (1:1000 dilution; Sigma-Aldrich), anti-phospho-JNK (1:1000; Cell Signaling Tech., Danvers, MA), anti-JNK (1:1000; Cell Signaling Tech.), anti-phospho-p38 MAPK (1:1000, Cell Signaling Tech.), anti-p38 MAPK (1:1000, Cell

Signaling Tech.), anti-phospho-ERK (1:1000, Cell Signaling Tech.), anti-ERK (1:1000, Cell Signaling Tech.), anti-phospho-p65 (1:1000, Cell Signaling Tech.), anti-p65 (1:1000, Cell Signaling Tech.), anti-UPF1 (1:1000; Bethyl Laboratories, Montgomery, TX), or anti-GAPDH (1:5000; Santa Cruz Biotech., Santa Cruz, CA) antibody.

*Immunohistochemistry*. HCT116 cells growing on a multichamber culture slide (Matsunami Glass Ind., Osaka, Japan) were rinsed briefly in phosphate-buffered saline (PBS) and then fixed in 4% paraformaldehyde in PBS for 10 min at room temperature. The fixed cells were permeabilized in PBS containing 0.1% Triton X-100 for 10 min. After blocking with 4% Block Ace (Snow Brand Milk Products Co., Tokyo, Japan) at room temperature for 1 h, slides were incubated overnight at 4ºC with a mouse anti-FLAG (1:2000 dilution, Sigma-Aldrich) and a rabbit anti-TIAR (1:1600, Cell Signaling Tech.) antibodies in PBS containing 1% Block ACE and 0.1% TritonX-100. After washing, the slides were treated with a 1:1000 dilution of Alexa Fluor 488-conjugated anti-mouse IgG (Invitrogen) and a 1:1000 dilution of Alexa Fluor 555-conjugated anti-rabbit IgG. Nuclei were counterstained with TO-PRO-3 (Molecular Probes, Eugene, OR). After washing, the slides were mounted in Vectashield mounting medium (Vector Labo., Burlingame, CA) and examined by a confocal laser-scanning microscopy (FluoView FV1000; Olympus, Tokyo, Japan). Signal intensities of anti-c-JUN reactive bands were quantified using Image J software (http://www.rsb.info.nih.gov/ij/).

*Promoter activity assay*. The 5′ flank of the human *IL-8* gene was cloned into the pGL3-basic luciferase reporter vector (Promega). In brief, the first PCR was performed using human genomic DNA as a template. The *IL-8* proximal promoter region (from -652 to +46 bp) was amplified using the following primer set:
5’-AAAAAGGTACCTAGTCTTATCTATTTCTAGATC-3’ (forward) and

5’-AAAAAGAGCTCGAAGCTTGTGTGCTCTGCTGTC-3’ (reverse). Subsequently, the amplified product was used as a template to generate deletion constructs consisting of the -229 to +46 bp, -99 to +46 bp, and -55 to +46 bp regions using the same reverse primer and one of the following forward primers:
5’-AAAAAGGTACCGAGCTTCAGTATTTTAAATGTATA-3’ for -229 to +46 bp,
5’-AAAAAGGTACCGCCATCAGTTGCAAATCGTG-3’ for -99 to +46 bp and
5’-AAAAAGGTACCAGGGTGCATAAGTTCTCTAGTAG-3’ for -55 to +46 bp. The amplified products were subcloned into the pGL3-basic vector using KpnI and SacI restriction sites. To generate a mutated reporter plasmid directed the activator protein-1 (AP-1), PCR was performed using a KOD-Plus-Mutagenesis Kit (TOYOBO) and pGL3 -229/+46 as the template. The two-point mutation in the AP-1 binding site (-126 TGACTCA -120 bp to -126 TATCTCA -120 bp) were prepared from pGL3 -229/+46 construct. To generate AP-1 reporter vector (pGL3-AP1), minimal promoter (minP) sequence;
5’-AGACACTAGAGGGTATATAATGGAAGCTCGACTTCC-3’ were subcloned into the pGL3-basic vector using restriction sites. Subsequently, AP-1 response elements;
5’-TGAGTCAGTGACTCAGTGAGTCAGTGACTCAGTGAGTCAGTGACTCAG- 3’ was subcloned into the pGL3-minP. pGL3-minP was used as a negative promoter activity. HCT116 cells ($2.0 \times 10^4$ cells) were cultured on 24-well plates, and then pGL-3 luciferase constructs (100 ng) were co-transfected with pRL-CMV vector (50 ng) using FuGENE HD (Promega). Twenty-four hours after the transfection, cells were harvested, and the firefly and renilla luciferase activities were measured using the Dual-Luciferase Reporter Assay System (Promega).

*Electrophoretic mobility shift assay (EMSA).* Nuclear proteins were prepared from HCT116 cells as previously described (17). A double-stranded oligonucleotide for the AP1 consensus binding site (-132 to -108 bp, GTGTGATGACTCAGGTTTGCCCTGA ) was

radiolabeled by filling in a 5' overhang with [α-$^{32}$P]deoxycytidine 5'-triphosphate and Klenow fragment (New England Biolabs, Beverly, MA) and then purified using a QIAquick nucleotide removal kit (Qiagen). A mutated probe for the AP1 site (AP1mt; GTGTGATATCTCAGGTTTGCCCTGA) was used as a non-self-competitor. Protein-DNA binding reactions were performed with 5 μg of nuclear extract proteins, 1 μl of $^{32}$P-labeled oligonucleotide (40,000 cpm), and 2 μg of salmon sperm DNA (Invitrogen) in 10 μl of 10 mM Tris·HCl buffer (pH 7.9) containing 50 mM NaCl, 5 mM $MgCl_2$, 10 mM EDTA, 10 mM DTT, and 20% glycerol. After being incubated at room temperature for 30 min, protein-DNA complexes were resolved on a 5% non-denaturing polyacrylamide gel in 0.25 × Tris-borate-EDTA buffer at 4°C. For self-competition experiments, the nuclear proteins were incubated with the unlabeled double-stranded oligonucleotide for 20 min at room temperature before addition of the $^{32}$P-labeled probe. Antibody perturbation experiments were performed by preincubating nuclear proteins with 1 μg of anti-c-JUN antibody for 30 min at room temperature before adding the $^{32}$P-labeled probe.

*Chromatin immunoprecipitation (ChIP) assay*. ChIP assays were performed using the Chromatin Immunoprecipitation Assay Kit (Millipore, Billerica, MA). Briefly, HCT116 cells were fixed with 1% formaldehyde in PBS for 10 min and then washed twice with ice-cold PBS. These cells were re-suspended in SDS lysis buffer, incubated for 10 min on ice, and then sonicated (Cell Signaling Tech.). Immunoprecipitation was carried out overnight at 4°C using 3 μg of anti-c-JUN antibody. Normal rabbit IgG was used to detect non-specific reactions. Immune complexes were collected with protein A agarose/salmon sperm DNA. Cross linking between proteins and DNA was reversed according to the manufacturer's protocol. Protein-bound DNA was extracted with phenol/chloroform/isoamyl alcohol. The extracted DNA was amplified by PCR (32 cycles; denaturing at 98°C for 10 s, annealing at 55°C for 30 s, and extension at 72°C for 1 min) using the following primers: for *IL-8*

sequence between -568 and -401 bp, 5'-ATGTGCCCCTTCACTCTGTT-3' and 5'-GGTGAAGATAAGCCAGCCAAT-3'; for *IL-8* sequence between -263 and -111 bp, 5'-AAAAAGCATACAATTGATAATTCACC-3' and 5'-GGCAAACCTGAGTCATCACA-3'. The nuclear chromatin DNA from HCT116 cells (input) was used as a positive control for PCR.

## RESULTS

*Production of SRSF3-PTC mRNA isoform after exposure to sodium arsenite. SRSF3* generates two mRNA isoforms through alternative splicing, a major isoform (we describe here as *SRSF3-FL*) and a minor isoform (*SRSF3-PTC*) (Fig. 1*A*). When HCT116 cells were exposed to 100 μM arsenite or 500 μM hydrogen peroxide ($H_2O_2$) for 6 h, they significantly increased *SRSF3-PTC* mRNA levels without changing *SRSF3-FL* mRNA levels (Fig. 1*B*). Pretreatment with an antioxidant N-acetyl-cysteine pretreatment (NAC, 10 mM) almost completely blocked both arsenite- and $H_2O_2$-stimulated *SRSF3-PTC* mRNA expression, suggesting that oxidative stress stimulates production of *SRSF3-PTC* mRNA isoform (Fig. 1*B*). After treatment of HCT116 cells with 100 μM sodium arsenite, *SRSF3-PTC* mRNA levels were increased with a peak at 3 h, and remained to be elevated for at least 12 h without changing *SRSF3-FL* mRNA levels (Fig. 2*A*). The arsenite-stimulated production of *SRSF3-PTC* mRNA through alternative splicing was also detectable by RT-PCR using the primer set designed to amplify the exons 3-5 (Fig. 2*B*). *SRSF3-PTC* mRNA should be degraded through NMD. At the same time, however, it was possible that *SRSF3-PTC* mRNA expressed in arsenite-treated cells would be translated into a truncated protein partially lacking of the RS domain (SRSF3-TR) (Fig. 1*A*). Western blotting using an antibody against the N-terminus of SRSF3 showed that treatment of HCT116 cells with arsenite newly induced

an immunoreactive protein with a predicted molecular size of SRSF3-TR (14 kDa), while it did not increase levels of constitutive, full-length SRSF3 protein (SRSF3-FL) (Fig. 2*C*). Treatment with *SRSF3-PTC* siRNA specifically targeting *SRSF3* exon 4 completely blocked the arsenite-induced appearance of the immunoreactive protein band (Fig. 2*D*), indicating that the 14 kDa protein was likely to be SRSF3-TR.

*NMD-mediated degradation of SRSF3-PTC mRNA.* mRNAs containing PTCs that are located more than 50 nucleotides upstream of the final exon-exon junction are considered to be targets for NMD (26). To examine whether *SRSF3-PTC* mRNA is actually regulated by NMD, we first disrupted NMD by knockdown of UPF1, which is an essential factor of NMD pathway (29). Reduction of UPF1 after treatment with *UPF1* siRNA for 48 h (Fig. 3*A*) increased *SRSF3-PTC* mRNA levels 4-fold (Fig. 3*B*). Inhibition of NMD by treatment with cycloheximide also increased *SRSF3-PTC* mRNA levels 30-fold (Fig. 3*C*). Thus, *SRSF3-PTC* mRNA appeared to be a target for NMD. It has been shown that NMD is often inactivated under stressful conditions including hypoxia, amino acid starvation, and oxidative stress (8, 27, 35). Exposure to arsenite was also reported to inhibit NMD activity in mouse embryonic fibroblasts (MEFs) and Chinese hamster ovary (CHO) cells (35). To test whether arsenite inhibited NMD activity in HCT116 cells, we employed a chemiluminescence-based reporter system (3). Plasmids containing a fusion construct of an in-frame *Renilla* luciferase and human *β-globin* gene with or without a nonsense mutation at codon 39 (NS39 or WT, respectively) (25, 33) were co-transfected with firefly luciferase served as a normalization control. NMD activity was monitored as the ration between NS39 and WT chemiluminescences. As shown in Fig. 3*D*, after treatment with arsenite, relative luciferase activity (NS39/WT) was significantly increased probably due to impaired degradation of the nonsense-mutated human *β-globin* (NS39) transcripts by NMD. In fact, in the presence of a transcription inhibitor actinomycin D (2.5 μg/ml), a half-life of *SRSF3-PTC* mRNA became

longer to > 8 h in arsenite-treated cells, compared with around 2 h of a half-life in untreated control cells (Fig. 3*E*)

*Subcellular distribution of SRSF3-PTC mRNA isoform.* Although several models for the mechanism of NMD have been proposed (30), a pioneer round of translation in the cytoplasm is an essential step for recognition of PTC-containing mRNAs by NMD. Thus, NMD degrades PTC-containing mRNAs mainly in the cytoplasm. Nuclear and cytoplasmic fractions were prepared before (0) or 3 and 6 h after treatment with arsenite, and the purity of each fraction was confirmed by RT-PCR using the primer set for *GAPDH* pre-mRNA (Fig. 4*A*). In cytoplasmic fractions, an exon 4-containing transcript (*SRSF3-PTC*) appeared 3 h after exposure to arsenite, and its levels time-dependently increased (Fig. 4*A*). In nuclear fractions, *SRSF3-PTC* mRNA was present before arsenite treatment, and its levels were not changed after exposure to arsenite (Fig. 4*A*). The time-dependent changes in subcellular distribution of *SRSF3-PTC* mRNA were quantified by qPCR (Fig. 4*B*). qPCR demonstrated that treatment with arsenite increased *SRSF3 PTC* mRNA levels preferentially in the cytoplasm (20-fold increase), compared with those in the nucleus (less than 2-fold increase) (Fig. 4*B* and *C*). These results suggested that in the presence of arsenite, *SRSF3-PTC* mRNA appeared to escape from degradation through the NMD system, and significant amounts of *SRSF3-PTC* mRNA were accumulated in the cytoplasm. As a consequence, SRSF3-TR could be transiently translated from *SRSF3-PTC* mRNA under oxidative stress.

*Phosphorylation and subcellular localization of SRSF3-TR*. Phosphorylation of RS domain determines the subcellular localization of individual SR proteins (5, 21). It has been shown that functional SRSF3-FL localizes in the nuclear speckles (4, 23). We next examined phosphorylation and subcellular localization of SRSF3-TR partially lacking RS domain. Since the anti-SRSF3 antibody used was raised against the N-terminus of SRSF3, it could not

distinguish between SRSF3-TR and SRSF3-FL. We therefore transfected plasmids encoding *FLAG-tagged-SRSF3-FL* or *-PTC* and assessed phosphorylation of SRSF3-TR and SRSF3-FL by Western blotting using the anti-SRSF3 and an anti-FLAG antibodies (Fig. 5). The anti-FLAG antibody recognized FLAG-SRSF3-FL and -TR. Dephosphorylated FLAG-SRSF3-FL and endogenous SRSF3-FL appeared after a calf intestinal phosphatase (CIP) treatment, while we could not detect any shifted band of FLAG-SRSF3-TR after CIP treatment (Fig. 5, upper panel). Endogenous SRSF3-TR was not detectable with the anti-SRSF3 antibody in mock-, *FLAG-SRSF3-FL*-, or *FLAG-SRSF3-TR*-transfected cells, and the anti-SRSF3 antibody recognized the dephosphorylation of endogenous or FLAG-tagged SRSF3-FL in these cells (Fig. 5, middle panel).

To examine the subcellular localization of SRSF3-FL and SRSF3-TR, we performed double-immunofluorostaining with an antibody to FLAG and an antibody to a stress granule-associated TIAR protein using FLAG-SRSF3-FL- or -TR-overexpressing HCT116 cells. Confocal laser-scanning microscopy showed that FLAG-SRSF3-FL was localized in nuclei (Fig. 6e), and a part of FLAG-SRSF3-FL was translocated to stress granules that appeared in the cytoplasm 6 h after exposure to arsenite (Fig. 6h'). In contrast, FLAG-SRSF3-TR was diffusely distributed in both the nucleus and the cytoplasm (Fig. 6i). At the same time, overexpression of FLAG-SRSF3-TR itself induced formation of stress granules in unstressed HCT116 cells (Fig. 6j), and a part of FLAG-SRSF3-TR was associated with them (Fig. 6l). After arsenite treatment, SRSF3-TR still remained in both stress granules and nucleus (Fig. 6l').

*Effect of SRSF3-TR on arsenite-stimulated IL-8 production.* It has recently been shown that SRSF3 acts as a negative regulator of inflammation (28). We also examined whether reduction of SRSF-TR changed expression of mRNAs encoding *IL-1β*, *IL-6*, *IL-8*, *interferon (IFN)-γ*, and *tumor necrosis factor (TNF)-α* after exposure to arsenite using qPCR, and found

that arsenite-stimulated elevation of *IL-8* mRNA levels was significantly attenuated in *SRSF3-PTC* siRNA-treated cells, compared with control siRNA-treated cells (Fig. 7*A*). Consequently, *SRSF3-PTC* siRNA significantly decreased arsenite-stimulated IL-8 release (Fig. 7*B*).

The human *IL-8* gene promoter contains a number of regulatory *cis* elements which are activated by the interaction with AP-1, CCAAT/enhancer-binding protein (C/EBP), and nuclear factor κB (NFκB) (15). The transcription start site of the *IL-8* gene is located on 101-bp upstream of the translation site. To define the minimal promoter of the *IL-8* gene responsive for arsenite stress, we generated the luciferase reporter vector having the 5'-flank of the human *IL-8* gene from -652 to +46 bp, and then serially truncated fragments were constructed. As shown in Fig. 7*C*, the arsenite-dependent luciferase activity resided in the proximal promoter region from -229 to -99 bp. This region contains an AP-1-binding site, and the two-point mutation of this AP-1 site almost completely inhibited the arsenite-dependent promoter activity (Fig. 7*C*), indicating a crucial role of AP-1 and its binding site located in -126 to -120 bp for arsenite-induced *IL-8* transcription. We also confirmed that *SRSF3-PTC* siRNA did not change the stability of *IL-8* mRNA (Fig. 7*D*), suggesting that *SRSF3-PTC* siRNA might down-regulate transcription of the *IL-8* gene.

As shown in Fig. 8, *SRSF3-PTC* siRNA did not significantly change levels of *IL-1β*, *IL-6*, *IFN-γ*, and *TNF-α* mRNAs before and after treatment with arsenite. We also examined whether SRSF3-PTC siRNA affected survival or apoptosis after exposure to higher concentrations of arsenite, but we could not detect any changes in numbers of viable cells and terminal deoxynucleotidyl transferase-mediated dUTP nick-end labeling-positive cells between SRSF3-PTC or control siRNA-treated cells (data not shown).

*Effect of SRSF3-PTC siRNA on arsenite-stimulated c-JUN protein induction*. AP-1 is a homo- or heterodimer composed of the Jun and Fos family members. Among them, c-JUN

and c-Fos together comprise an AP-1 heterodimer and induce *IL-8* gene transcription (34). Mitogen-activated protein kinases (MAPKs), including the extracellular-regulated protein kinase (ERK), JUN-N-terminal protein kinase (JNK), and p38 MAPK are involved in the *IL-8* gene transcription (11). As shown in Fig. 9*A* and *B*, the induction of c-JUN protein was significantly reduced 3, 6, and 9 h after exposure to arsenite in SRSF3-PTC siRNA-treated cells, compared with that in control siRNA-treated cells. There were no differences in expression and phosphorylation of p38 MAPK, ERK, or c-Fos between *SRSF3-PTC* and control siRNA-treated cells (Fig. 9*A*). We also investigated the possibility that changes in NFκB activation were involved in the attenuation of the *IL-8* gene transcription in *SRSF3-PTC* siRNA-treated cells. We compared phosphorylation of an essential factor of NFκB (p65), and confirmed that *SRSF3-PTC* knockdown did not change p65 phosphorylation after exposure to arsenite (Fig. 9*A*). These results suggested that the reduction of c-JUN protein might be responsible for the down-regulation of arsenite-stimulated *IL-8* gene transcription in *SRSF3-PTC* siRNA-treated cells.

*Reduction of c-JUN binding to IL-8 promoter in SRSF3-PTC siRNA-treated cells.*

To determine whether the AP-1 consensus sequence (TGACTCA) located at -126 and -120 bp in the 5′-flanking region was able to interact with c-JUN, we synthesized a 25-bp double-stranded oligonucleotide (−132 to −108 bp;GTGTGATGACTCAGGTTTGCCCTGA) and used it as a probe for electrophoretic mobility shift assay. As shown in Fig. 10*A*, arsenite stress for 3 h strongly generated a complex that was weakly induced in cell lysates from cells not treated with arsenite, and *SRSF3-PTC* siRNA treatment reduced this arsenite-induced complex. Unlabeled self-oligonucleotide, but not the mutated AP-1 oligonucleotide (GTGTGATATCTCAGGTTTGCCCTGA), competed for formation of this complex. Moreover, preincubation with an anti-cJUN antibody, but not rabbit IgG, supershifted this band and produced a more slowly migrated band (Fig. 10*A*). Together, these results indicate

that arsenite stress produced an interaction between activated c-JUN and the AP-1 binding element present in the 5′-flanking region of the human *IL-8* gene.

To confirm the results obtained from EMSA and to reveal a crucial role of c-JUN in the reduction of *IL-8* transcription, chromatin immunoprecipitation (ChIP) assay was employed using an anti-c-JUN antibody. As shown in Fig. 10*B*, c-JUN bound to the -263/-111 bp region containing an AP-1 binding site in both control and *SRSF3-PTC* siRNA-treated cells, whereas c-JUN did not bind to the -568/-401 bp region. As expected, exposure to arsenite increased the binding of c-JUN in both control and *SRSF3-PTC* siRNA-treated cells. qPCR measurement of the immunoprecipitated -263/-111 bp region demonstrated that arsenite-induced c-JUN binding to the *IL-8* promoter was partially, but significantly attenuated in *SRSF3-PTC* siRNA-treated cells (Fig. 10*C*).

AP-1 binding sites are widely found in promoter regions of various genes, especially related to proliferation, apoptosis, survival, and tumorigenesis. AP-1 reporter assay was employed to examine whether *SRSF-PTC* siRNA generally affected AP-1 activity. As shown in Fig. 10*D*, treatment of HCT116 cells with *SRSF3-PTC* siRNA significantly inhibited arsenite-stimulated AP-1 reporter activity, suggesting that SRSF3-TR might modify AP-1-dependent cellular stress responses.

## DISCUSSION

Alternative splicing generates protein isoform diversity and profoundly affects gene expression program. However, up to one-third of human alternative splicing events generate a PTC that would cause the resulting mRNA to be degraded by NMD (20), indicating the widespread coupling of alternative splicing and NMD (AS-NMD). Interestingly, AS-NMD events are found in all SR-protein genes including *SRSF3* (19). Furthermore, these events

coincide with regions of extreme sequence conservation, termed “ultraconserved elements” (UCEs), suggesting the existence of evolutional significance of UCEs. There are 481 described UCEs, and 68% of them are transcribed, constituting a new category of non-coding RNAs (6). However, 47% of UCEs have been designated either exonic or probably exonic (2). *SRSF3* gene contains a 577-bp UCE that includes entire exon 4 (Supplementary Fig. S1 for reviewers). We found that sodium arsenite stimulated cytoplasmic accumulation of *SRSF3-PTC* mRNA isoform through inhibition of NMD activity, resulting in translation of a truncated protein, SRSF3-TR, in colon cancer cells (HCT116). Furthermore, arsenite stress facilitated nuclear translocation of SRSF3-TR, suggesting novel function(s) of the truncated protein in the nucleus under oxidative stress.

Jumaa and Nielsen reported that SRSF1 (also known as ASF/SF2) and SRSF2 (SC35) were involved in the exclusion of *SRSF3* exon 4 (13, 14). The inclusion of exon 4 to mature SRSF3 mRNA was reported to occur under serum starvation (12), and the biological significance of exon 4-inclusion is considered to be an auto-regulatory feedback loop by SRSF3 itself (13). Moreover, because of multiple PTCs in the exon 4, a recent study (19) together with our findings have revealed that exon 4-including *SRSF3-PTC* mRNA is a target for NMD. To avoid production of the C-terminally truncated proteins which have potential dominant-negative or gain-of-function, PTC-containing mRNAs are expected to be degraded by NMD. However, several lines of evidence have shown that NMD activity is often inhibited by stresses, such as hypoxia, amino acid starvation, and generation of reactive oxygen species (8, 27, 35). Consistent with those reports, our results also suggest that the cytoplasmic accumulation of *SRSF3-PTC* mRNA may, at least in part, result from inhibition of NMD under arsenite-induced oxidative stress. In addition, expression of PTC-containing mRNA isoforms of other SR protein genes (*SRSF6*, *SRSF7* and *SRSF9*) were also up-regulated after exposure to arsenite (data not shown), suggesting that arsenite stress may extensively modify AS-NMD events. Arsenite stress may also change alternative splicing pattern to preferentially

produce *SRSF3-PTC* variant. To address this issue, we prepared a minigene spaninig *SRSF3* exon 2 to exon 7. This minigene produced exon 4-containing transcript as a major transcript, and we could not detect any change in alternative splicing. Truncated SRSF3 is translated from cytosolic *SRSF3-PTC* mRNA. Arsenite increased *SRSF3-PTC* mRNA levels 20-fold in the cytoplasmic fractions (Fig. 4*B* and *C*), while it did not change the major isoform (*SRSF3-FL* mRNA) levels (Fig. 2*A*). Arsenite treatment apparently stabilized *SRSF3-PTC* mRNA (Fig. 3*E*). These results suggest that regulation of mRNA stability may play an important role in the arsenite-induced accumulation of truncated SRFS3 protein.

Overexpression of SRSF3-TR alone could induce stress granule formation. Interestingly, a part of SRSF3-TR was co-localized with a stress granule marker TIAR. It was reported that SRSF3-ΔRS protein lacking entire RS domain localized throughout the cytoplasm and nucleoplasm (4), suggesting that RS domain has a crucial role in determining subcellular localization. In that case, stress-granule formation was not documented (4). SRSF3-TR still has partial RS domain, which might be responsible for stress granules formation in the cytoplasm. Stress granules are formed to protect RNAs from various types of stressors, such as oxidants or heat shock. The stress granule formation itself may modify the subsequent stress responses including the arsenite-induced IL-8 production. It is possible that the ability of the SRSF3-TR construct to induce stress granules may be important for understanding the role of this protein. Further studies are needed to clarify this issue.

To disclose unknown functions of SRSF3-TR, we focused on pro-inflammatory cytokine responses to arsenite, since silencing of *SRSF3* was reported to increase IL-1β secretion due to elevation of *IL-1β* and *caspase-1* mRNA levels in addition to activation of caspase-1 (28). SRSF3-TR knockdown did not affect arsenite-stimulated expression of *IL-1β*, *IL-6*, *IFN-γ*, and *TNF-α* mRNAs, but it significantly suppressed arsenite-stimulated elevation of *IL-8* mRNA levels and IL-8 release from HCT116 cells. IL-8 belongs to the C-X-C chemokine family and has proinflammatory effects. It has been shown that maximal IL-8

production requires combination of derepression of the gene promoter, activation of protein kinase cascades (JNK, p38 MAPK, ERK, and NFκB), and enhanced mRNA stabilization and translation efficiency (11). Among these regulators, AP-1 was found to be crucial for arsenite-stimulated promoter activity of the *IL-8* gene in HCT116 cells. Furthermore, we found that SRSF3-TR knockdown decreased arsenite-stimulated c-JUN induction. Consistent with the reduction of c-JUN protein levels, EMSA and ChIP assay experiments also showed that SRSF3-TR knockdown partially inhibited the binding of the cJUN/AP1 complex to the AP-1-binding element. RNA-immunoprecipitation (RNA-IP) showed that SRSF3-TR bound to *JUN* mRNA, suggesting a possibility that SRSF3-TR may alter *JUN* mRNA stability. However, we could not detect any difference in the stability between control and *SRSF3-PTC* siRNA-treated cells (data not shown). To further investigate this issue, we established a cell line stably expressing FLAG-SRSF3-TR. Consistent with the results obtained in *SRSF3-PTC* siRNA-treated cells, c-JUN protein levels were significantly increased in FLAG-SRSF3-TR-overexpressing cells. Similarly, there was no difference in *JUN* mRNA stability between the FLAG-SRSF3-TR-expressing cell line and control cells (data not shown). The present study suggests that SRSF3-TR knockdown reduces arsenite-induced IL-8 production, at least in part, through regulation of c-JUN protein levels. Once c-JUN/AP1 is activated, c-JUN is positively autoregulated by its product, cJun/AP-1 (1). Although it is still unknown what an initiator of c-JUN/AP1 activity is and how SRSF3-TR interacts with it, we have provided the first evidence that a functional truncated SR protein could be translated from an UCE- and PTC-containing splice variant of the SR protein family gene.

Finally, as mentioned above, NMD was often inhibited under certain condition such as hypoxia and oxidative stress. Cancer tissues are exposed to similar microenviromental conditions, and it has been shown that the impairment of NMD is involved in the oncogenic mechanism (9). In such situations, oxidative stress-induced SRSF3-TR might function as a potential mediator of inflammation. Further studies are needed to fully elucidate the

molecular mechanism for the SRSF3-TR-dependent regulation of c-JUN expression. Although UCEs are considered to have evolutional importance, their biological significance is not fully understood. Our finding may provide a new insight of UCEs encoded in the SR protein family genes.

## CONFLICTS OF INTEREST

The authors declare no conflict of interest.

## ACKNOWLEDGEMENTS

We thank Dr. Andreas E. Kulozik (University of Heidelberg) for providing plasmids of pCI-neo β-globin WT and NS39, and pCI-neo firefly.

## GRANTS

This work was supported by the grant from the Takeda Science Foundation (to K.N.) and the Grants-in-Aid for Scientific Research from the Ministry of Education, Culture, Sports, Science and Technology, Japan (#12016603 to K.N. and #22390146 to K.R.).

**REFERENCES**


1. **Angel, P., K. Hattori, T. Smeal, and M. Karin.** The jun proto-oncogene is positively autoregulated by its product, Jun/AP-1. *Cell* 55:875-85, 1988.
2. **Bejerano, G., C. B. Lowe, N. Ahituv, B. King, A. Siepel, S. R. Salama, E. M. Rubin, W. J. Kent, and D. Haussler.** A distal enhancer and an ultraconserved exon are derived from a novel retroposon. *Nature* 441:87-90, 2006.
3. **Boelz, S., G. Neu-Yilik, N. H. Gehring, M. W. Hentze, and A. E. Kulozik.** A chemiluminescence-based reporter system to monitor nonsense-mediated mRNA decay. *Biochem Biophys Res Commun* 349:186-91, 2006.
4. **Caceres, J. F., T. Misteli, G. R. Screaton, D. L. Spector, and A. R. Krainer.** Role of the modular domains of SR proteins in subnuclear localization and alternative splicing specificity. *J Cell Biol* 138:225-38, 1997.
5. **Caceres, J. F., G. R. Screaton, and A. R. Krainer.** A specific subset of SR proteins shuttles continuously between the nucleus and the cytoplasm. *Genes Dev* 12:55-66, 1998.
6. **Calin, G. A., C. G. Liu, M. Ferracin, T. Hyslop, R. Spizzo, C. Sevignani, M. Fabbri, A. Cimmino, E. J. Lee, S. E. Wojcik, M. Shimizu, E. Tili, S. Rossi, C. Taccioli, F. Pichiorri, X. Liu, S. Zupo, V. Herlea, L. Gramantieri, G. Lanza, H. Alder, L. Rassenti, S. Volinia, T. D. Schmittgen, T. J. Kipps, M. Negrini, and C. M. Croce.** Ultraconserved regions encoding ncRNAs are altered in human leukemias and carcinomas. *Cancer cell* 12:215-29, 2007.
7. **Chen, M., and J. L. Manley.** Mechanisms of alternative splicing regulation: insights from molecular and genomics approaches. *Nat Rev Mol Cell Biol* 10:741-54, 2009.
8. **Gardner, L. B.** Hypoxic inhibition of nonsense-mediated RNA decay regulates gene expression and the integrated stress response. *Mol Cell Biol* 28:3729-41, 2008.
9. **Gardner, L. B.** Nonsense-mediated RNA decay regulation by cellular stress: implications for tumorigenesis. *Mol Cancer Res* 8:295-308, 2010.
10. **He, X., A. D. Arslan, M. D. Pool, T. T. Ho, K. M. Darcy, J. S. Coon, and W. T. Beck.** Knockdown of splicing factor SRp20 causes apoptosis in ovarian cancer cells and its expression is associated with malignancy of epithelial ovarian cancer. *Oncogene* 30:356-365, 2011.
11. **Hoffmann, E., O. Dittrich-Breiholz, H. Holtmann, and M. Kracht.** Multiple control of interleukin-8 gene expression. *J Leukoc Biol* 72:847-55, 2002.
12. **Jumaa, H., J. L. Guenet, and P. J. Nielsen.** Regulated expression and RNA processing of transcripts from the Srp20 splicing factor gene during the cell cycle. *Mol Cell Biol* 17:3116-24, 1997.
13. **Jumaa, H., and P. J. Nielsen.** Regulation of SRp20 exon 4 splicing. *Biochim Biophys Acta* 1494:137-43, 2000.

14. **Jumaa, H., and P. J. Nielsen.** The splicing factor SRp20 modifies splicing of its own mRNA and ASF/SF2 antagonizes this regulation. *EMBO J* 16:5077-85, 1997.
15. **Khanjani, S., V. Terzidou, M. R. Johnson, and P. R. Bennett.** NFkappaB and AP-1 drive human myometrial IL8 expression. *Mediators Inflamm* 2012:504952, 2012
16. **Kurokawa, K., Y. Akaike, K. Masuda, Y. Kuwano, K. Nishida, N. Yamagishi, K. Kajita, T. Tanahashi, and K. Rokutan.** Downregulation of serine/arginine-rich splicing factor 3 induces G1 cell cycle arrest and apoptosis in colon cancer cells. *Oncogene*, 2013.
17. **Kuwano, Y., T. Kawahara, H. Yamamoto, S. Teshima-Kondo, K. Tominaga, K. Masuda, K. Kishi, K. Morita, and K. Rokutan.** Interferon-gamma activates transcription of NADPH oxidase 1 gene and upregulates production of superoxide anion by human large intestinal epithelial cells. *Am J Physiol Cell Physiol* 290:C433-43, 2006.
18. **Kuwano, Y., R. Pullmann, Jr., B. S. Marasa, K. Abdelmohsen, E. K. Lee, X. Yang, J. L. Martindale, M. Zhan, and M. Gorospe.** NF90 selectively represses the translation of target mRNAs bearing an AU-rich signature motif. *Nucleic acids research* 38:225-38, 2010.
19. **Lareau, L. F., M. Inada, R. E. Green, J. C. Wengrod, and S. E. Brenner.** Unproductive splicing of SR genes associated with highly conserved and ultraconserved DNA elements. *Nature* 446:926-9, 2007.
20. **Lewis, B. P., R. E. Green, and S. E. Brenner.** Evidence for the widespread coupling of alternative splicing and nonsense-mediated mRNA decay in humans. *Proc Natl Acad Sci U S A* 100:189-92, 2013.
21. **Li, S. J., Y. Qi, J. J. Zhao, Y. Li, X. Y. Liu, X. H. Chen, and P. Xu.** Characterization of Nuclear Localization Signals (NLSs) and Function of NLSs and Phosphorylation of Serine Residues in Subcellular and Subnuclear Localization of Transformer-2beta(Tra2beta). *J Biol Chem*, 2013.
22. **Lin, S., G. Coutinho-Mansfield, D. Wang, S. Pandit, and X.-D. Fu.** The splicing factor SC35 has an active role in transcriptional elongation. *Nat Struct Mol Biol* 15:819-826, 2008.
23. **Loomis, R. J., Y. Naoe, J. B. Parker, V. Savic, M. R. Bozovsky, T. Macfarlan, J. L. Manley, and D. Chakravarti.** Chromatin binding of SRp20 and ASF/SF2 and dissociation from mitotic chromosomes is modulated by histone H3 serine 10 phosphorylation. *Mol Cell* 33:450-61, 2009.
24. **Manley, J. L., and A. R. Krainer.** A rational nomenclature for serine/arginine-rich protein splicing factors (SR proteins). *Genes Dev* 24:1073-4, 2010.
25. **Maquat, L. E., A. J. Kinniburgh, E. A. Rachmilewitz, and J. Ross.** Unstable beta-globin mRNA in mRNA-deficient beta o thalassemia. *Cell* 27:543-53, 1981.
26. **McGlincy, N. J., and C. W. Smith.** Alternative splicing resulting in

nonsense-mediated mRNA decay: what is the meaning of nonsense? *Trends Biochem Sci* 33:385-93, 2008.

27. **Mendell, J. T., N. A. Sharifi, J. L. Meyers, F. Martinez-Murillo, and H. C. Dietz.** Nonsense surveillance regulates expression of diverse classes of mammalian transcripts and mutes genomic noise. *Nat Genet* 36:1073-8, 2004.
28. **Moura-Alves, P., A. Neves-Costa, H. Raquel, T. R. Pacheco, B. D'Almeida, R. Rodrigues, I. Cadima-Couto, A. Chora, M. Oliveira, M. Gama-Carvalho, N. Hacohen, and L. F. Moita.** An shRNA-based screen of splicing regulators identifies SFRS3 as a negative regulator of IL-1beta secretion. *PLoS One* 6**:**e19829, 2011.
29. **Nicholson, P., H. Yepiskoposyan, S. Metze, R. Zamudio Orozco, N. Kleinschmidt, and O. Muhlemann.** Nonsense-mediated mRNA decay in human cells: mechanistic insights, functions beyond quality control and the double-life of NMD factors. Cell *Mol Life Sci* 67:677-700, 2010.
30. **Palacios, I. M.** Nonsense-mediated mRNA decay: from mechanistic insights to impacts on human health. *Brief Funct Genomics* 12**:**25-36, 2013.
31. **Sanford, J. R., N. K. Gray, K. Beckmann, and J. F. Caceres.** A novel role for shuttling SR proteins in mRNA translation. *Genes Dev* 18:755-68, 2004.
32. **Sapra, A. K., M. L. Anko, I. Grishina, M. Lorenz, M. Pabis, I. Poser, J. Rollins, E. M. Weiland, and K. M. Neugebauer.** SR protein family members display diverse activities in the formation of nascent and mature mRNPs in vivo. *Mol Cell* 34:179-90, 2009.
33. **Thermann, R., G. Neu-Yilik, A. Deters, U. Frede, K. Wehr, C. Hagemeier, M. W. Hentze, and A. E. Kulozik.** Binary specification of nonsense codons by splicing and cytoplasmic translation. *EMBO J* 17:3484-94, 1998.
34. **Thompson, C., A. Cloutier, Y. Bosse, M. Thivierge, C. L. Gouill, P. Larivee, P. P. McDonald, J. Stankova, and M. Rola-Pleszczynski.** CysLT1 receptor engagement induces activator protein-1- and NF-kappaB-dependent IL-8 expression. *Am J Respir Cell Mol Biol* 35:697-704, 2006.
35. **Wang, D., J. Zavadil, L. Martin, F. Parisi, E. Friedman, D. Levy, H. Harding, D. Ron, and L. B. Gardner.** Inhibition of nonsense-mediated RNA decay by the tumor microenvironment promotes tumorigenesis. *Mol Cell Biol* 31:3670-80, 2011.

**FIGURE LEGENDS**

Fig. 1. Expression of the PTC-containg *SRSF3* (*SRSF3-PTC*) mRNA in HCT116 cells exposed to oxidative stress. (*A*) Schematic diagram of the SRSF3 gene and structures of SRSF3 proteins. Constitutive, functional SRSF3 protein (SRSF3-FL) is translated from *SRSF3-FL* mRNA isoform. *SRSF3* exon 4 contains multiple PTCs. The exon 4-containing mRNA isoform (*SRSF3-PTC)* is translated into a truncated protein, SRSF3-TR. (*B*) HCT116 cells were exposed to 100 μM sodium arsenite or 500 μM hydrogen peroxide for 6 h with or without 3-h pretreatment with an antioxidant N-acetyl-cysteine (NAC, 10 mM). Levels of *SRSF3-FL* and *SRSF3-PTC* mRNAs were measured by qPCR using *GAPDH* mRNA as an endogenous quantity control. Values are expressed as fold changes (means ± SD, n = 5) compared with the respective control values in untreated cells (0 h). *Significantly different by ANOVA and Scheffe's test ($P < 0.05$). PTC, premature termination codon; RRM, RNA recognition motif; RS, arginine/serine (RS)-rich domain.

Fig. 2. Expression of a truncated SRSF3 (SRSF3-TR) protein in HCT116 cells exposed to arsenite. (*A*) HCT116 cells were exposed to 100 μM sodium arsenite for the indicated times. Levels of *SRSF3-FL* (●) and *SRSF3-PTC* (□) mRNAs were measured by qPCR using *GAPDH* mRNA as an endogenous quantity control. Values are expressed as fold changes (means ± SD, n = 6) compared with the respective control values in untreated cells (0 h). *Significantly different by ANOVA and Scheffe's test ($P < 0.05$). (*B*) RT-PCR was performed to amplify exons 3-5 of *SRSF3*. Representative data are shown from three independent experiments. (*C*) Before (0 h) and at the indicated h after treatment with 100 μM sodium arsenite, amounts of SRSF3 proteins in whole-cell lysates were measured by Western blot analysis using an anti-SRSF3 antibody. GAPDH was used as a loading control. Representative data are shown from three independent experiments. (*D*) After treatment of

HCT116 cells with control or *SRSF3-PTC* siRNA for 24 h, they were exposed to 100 μM arsenite for 6 h. Amount of SRSF3 proteins were measured as in (*C*). Representative data are shown from three independent experiments.

Fig. 3. Effects of inhibition of NMD on *SRSF3-PTC* mRNA levels. (*A*) HCT116 cells were treated with 10 nM *UPF1* or control siRNA for 48 h. Amounts of UPF1 protein in these cells were measured by western blotting using GAPDH as a loading control. Representative data are shown from three independent experiments. (*B*) Levels of *SRSF3-FL* and *-PTC* mRNAs were also measured by qPCR in the siRNA-treated cells. Values are expressed as fold changes (means ± SD, n=3) *Significantly different ($P < 0.05$ by ANOVA and Scheffe's test). (*C*) HCT116 cells were incubated in the presence of cycloheximide (CHX, 50 or 100 μg/ml) for 6 h. Levels of *SRSF3-FL* and *-PTC* mRNAs were measured by qPCR. Values are expressed as fold changes (means ± SD, n=3) *Significantly different ($P < 0.05$ by ANOVA and Scheffe's test). (*D*) For measurement of chemiluminescence-based NMD activity, HCT116 cells were transfected with plasmids encoding WT or NS39 as described in "MATERIALS AND METHODS". They were exposed to 100 μM arsenite for the indicated times. Relative NS39 *Renilla* luciferase activity compared with WT was calculated. Co-expressed firefly luciferase activity was used to monitor transfection efficiency. Values are means ± SD, n=3. *Significantly different ($P < 0.05$ by ANOVA and Scheffe's test). (*E*) HCT116 cells were left untreated (●) or treated (■) with 100 μM arsenite for 3 h, and then they were incubated in the presence of actinomycin D (2.5 μg/ml) for the indicated times. Amounts of *SRSF3-PTC* mRNA remained were measured by qPCR.

Fig. 4. Subcellular distribution of *SRSF3-PTC* mRNA after arsenite treatment. (*A*) After treatment with 100 μM arsenite for the indicated times, subcellular fractions were prepared and subjected to RT-PCR analysis. *pre-GAPDH* mRNA was served as a specific marker for

nuclear fraction. Representative data are shown from three independent experiments. (*B*) and (*C*) *SRSF3-PTC* mRNA levels in each fraction were measured by qPCR using *GAPDH* mRNA as an endogenous quantity control. Values are means ± SD, n=5. *Significantly different by ANOVA and Scheffe's test ($P < 0.05$).

Fig. 5.Phosphorylation status of SRSF3-TR. Lysates of HCT116 cells transfected with mock, SRSF3-TR, or SRSF3-FL pCMV-3Tag plasmids were untreated or treated with calf intestine phosphatase (CIP) and subjected to Western blotting with an antibody against FLAG, SRSF3, or GAPDH. Phosphorylated (phospho) and de-phosphorylated (de-phospho) forms of SRSF3-FL are indicated. Representative data are shown from three independent experiments.

Fig.6. Subcellular localization of SRSF3-TR.

HCT116 cells were transfected with a plasmid encoding Flag-tagged SRSF3-FL ,SRSF3-TR, or mock. Before (control) or after exposure to 100 μM arsenite for 6 h, they were subjected to double-immunofluorescence staining using antibodies against FLAG (green) and TIAR (red), and then their nuclear were stained with TO-PRO3 (blue). Subcellular localization of FLAG-SRSF3-FL and FLAG-SRSF3-TR were visualized by a confocal laser-scanning microscopy (FluoView FV1000; Olympus). Representative data are shown from three independent experiments.

Fig. 7. Effects of *SRSF3-PTC* siRNA on arsenite-induced IL-8 expression. (*A*) After treatment of HCT116 cells with control (○) or *SRSF3-PTC* (■) siRNA for 24 h, they were exposed to 100 μM arsenite for the indicated times, *IL-8* mRNA levels were measured by qPCR using *GAPDH* mRNA as an internal quantity control. Values are expressed as fold changes (means ± SD, n=6). *Significantly different ($P < 0.05$ by ANOVA and Scheffe's test). (*B*) After treatment of HCT116 cells with the siRNAs as in (*A*), culture supernatants were collected and

subjected to measurement of IL-8 using an ELISA kit as described in "MATERIALS AND METHODS". Values are means ± SD, n=6. *Significantly different ($P < 0.05$ by ANOVA and Scheffe's test). (*C*) HCT116 cells were transfected with luciferase reporter plasmids (pGL3) driven by 652-, 229-, 99-, 55-bp *IL-8* promoter fragments or the two-point mutation of the AP-1 binding site (-126 bp) in a pGL3 -229/+46 construct. Twenty-four hours after transfection, HCT116 cells were harvested, and luciferase activity was measured using the Dual-Luciferase Reporter Assay System. Values are expressed as fold changes compared with pGL3-basic (mock) transfected cells. (means ± SD, n=6). *Significantly different by ANOVA and Scheffe's test ($P < 0.05$). (*D*) After treatment of HCT116 cells with control (○) or *SRSF3-PTC* (●) siRNA for 24 h, they were left untreated or treated with 100 μM arsenite for 3 h, and then they were incubated in the presence of 2.5 μg/ml actinomycin D for the indicated times. Amounts of *IL-8* mRNA were measured by qPCR at each time point.

Fig.8. Pro-inflammatory cytokines mRNA expression in *SRSF3-PTC* siRNA treated cells.(*A*) After treatment of HCT116 cells with control or *SRSF3-PTC* siRNA for 24 h, they were exposed to 100 μM arsenite for 6 h, levels of *IL-1β*, *IL-6*, *IFN-γ*, and *TNF-α* mRNA were measured by qPCR using *GAPDH* mRNA as an internal quantity control. Values are means ± SD, n=3. N.D., The indicated mRNAs were not detected.

Fig. 9. Effects of *SRSF3-PTC* siRNA on arsenite-induced induction and phosphorylation of MAPK- and NFκB-related molecules. (*A*) After treatment of HCT116 cells with control or *SRSF3-PTC* siRNA, they were exposed to 100 μM arsenite for the indicated times. Whole-cell lysates were prepared from them and subjected to Western blotting using the indicated antibodies. GAPDH was served as a loading control. Representative data are shown from four independent experiments. (*B*) Signal intensities of protein bands immunoreactive to anti-c-JUN antibody were assessed using NIH Image J software. Values are expressed as fold

changes using GAPDH as a loading control. Values are expressed as fold changes compared with untreated cells. (means ± SD, n=4). *Significantly different by ANOVA and Scheffe's test ($P < 0.05$).

Fig. 10. Effects of *SRSF3-PTC* siRNA on binding of c-JUN to the AP-1-binding site in the *IL-8* promoter. (A) Nuclear proteins were extracted from HCT116 cells treated without or with 100 μM sodium arsenite. Binding reactions between the nuclear proteins (5 μg) and 40,000 cpm of $^{32}$P-labeled double-stranded oligonucleotide of the AP-1-binding element were examined in the absence or presence of an excess of unlabeled AP-1 oligonucleotide (+, 2-fold; ++, 50-fold; +++, 200-fold excess) or a 150-fold molar excess of mutated AP-1 oligonucleotide (MT). For supershift experiments, nuclear extracts were preincubated with anti-cJUN antibody (1:50) for 30 min at room temperature before the $^{32}$P-labeled probe was added. An arrow indicates the supershifted (SS) DNA-protein complex and an arrowhead indicates cJUN-DNA complex. An asterisk indicates a non-specific spot. Representative data are shown from four independent experiments. (*B*) Schematic diagram of the human *IL-8* promoter and primer sets designed to amplify the indicated regions (primer sets 1 and 2). After treatment of HCT116 cells were left untreated or treated with 100 μM arsenite for 3 h, c-JUN binding to the *IL-8* promoter was assessed by chromatin-immunoprecipitaion (ChIP) analysis with an anti-c-JUN antibody as described in "MATERIALS AND METHODS". One percent of total input DNA was used as a loading control. Normal rabbit IgG was used to detect non-specific reactions for IP. RT-PCR analysis was done using primer sets specific for the *IL-8* promoter regions. Representative data are shown from three independent experiments. (*C*) Amounts of the AP-1-binding element immunoprecipitated with an anti-c-JUN antibody were measured qPCR using the *IL-8* primer set 2. Data are shown as amounts of bound AP-1-binding element in arsenite-treated cells relative to those in untreated control cells. Values are means ± SD, n=4. *Significantly different by ANOVA and Scheffe's test ($P < 0.05$).

Representative data are shown from three independent experiments. (*D*) After treatment of HCT116 cells with control or *SRSF3-PTC* siRNA for 24 h, they were transfected with a pGL3-AP1 or pGL3-minP (minP) reporter vector, and then incubated for another 24 h. These cells were left untreated or treated with 100 μM arsenite for 6 h, and then luciferase activity was measured using the Dual-Luciferase Reporter Assay System. Data are shown as arsenite-stimulated luciferase activity relative to that in untreated cells.

Fig. 1. *Kano et al.*

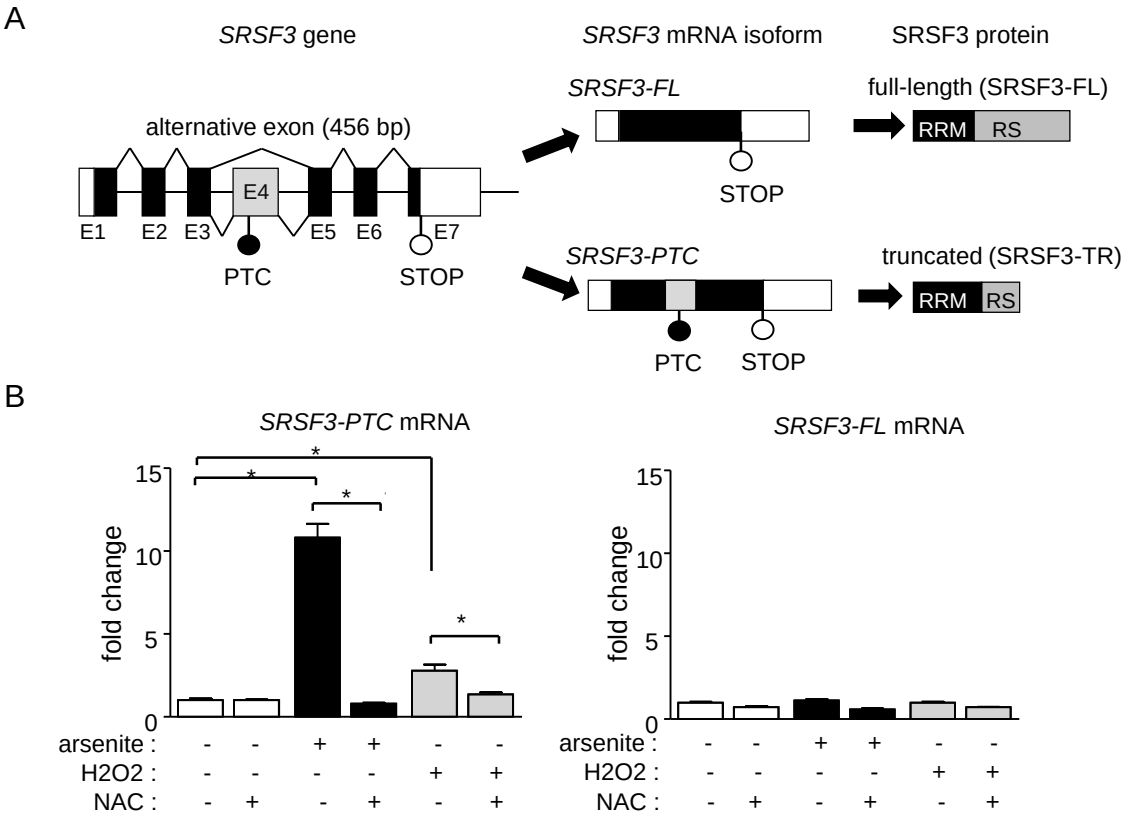

Fig. 2. *Kano et al.*

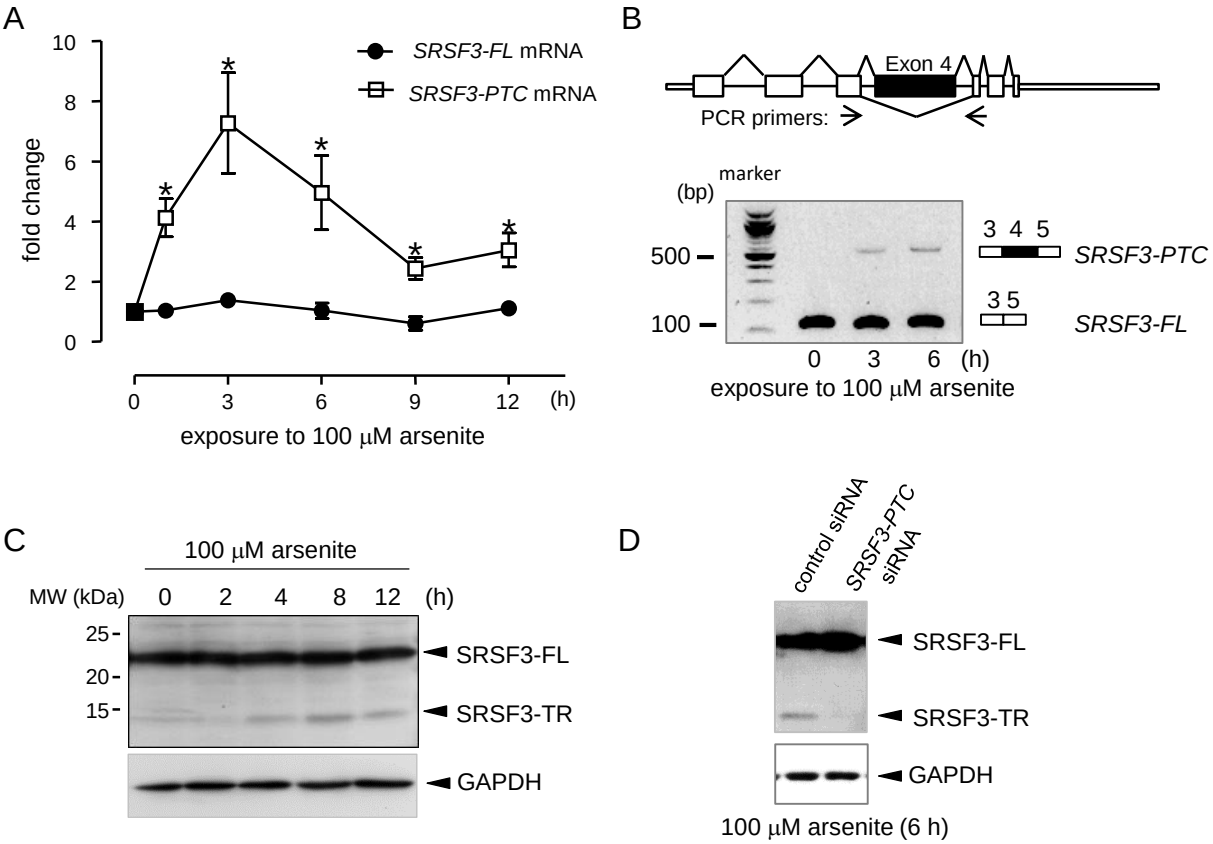

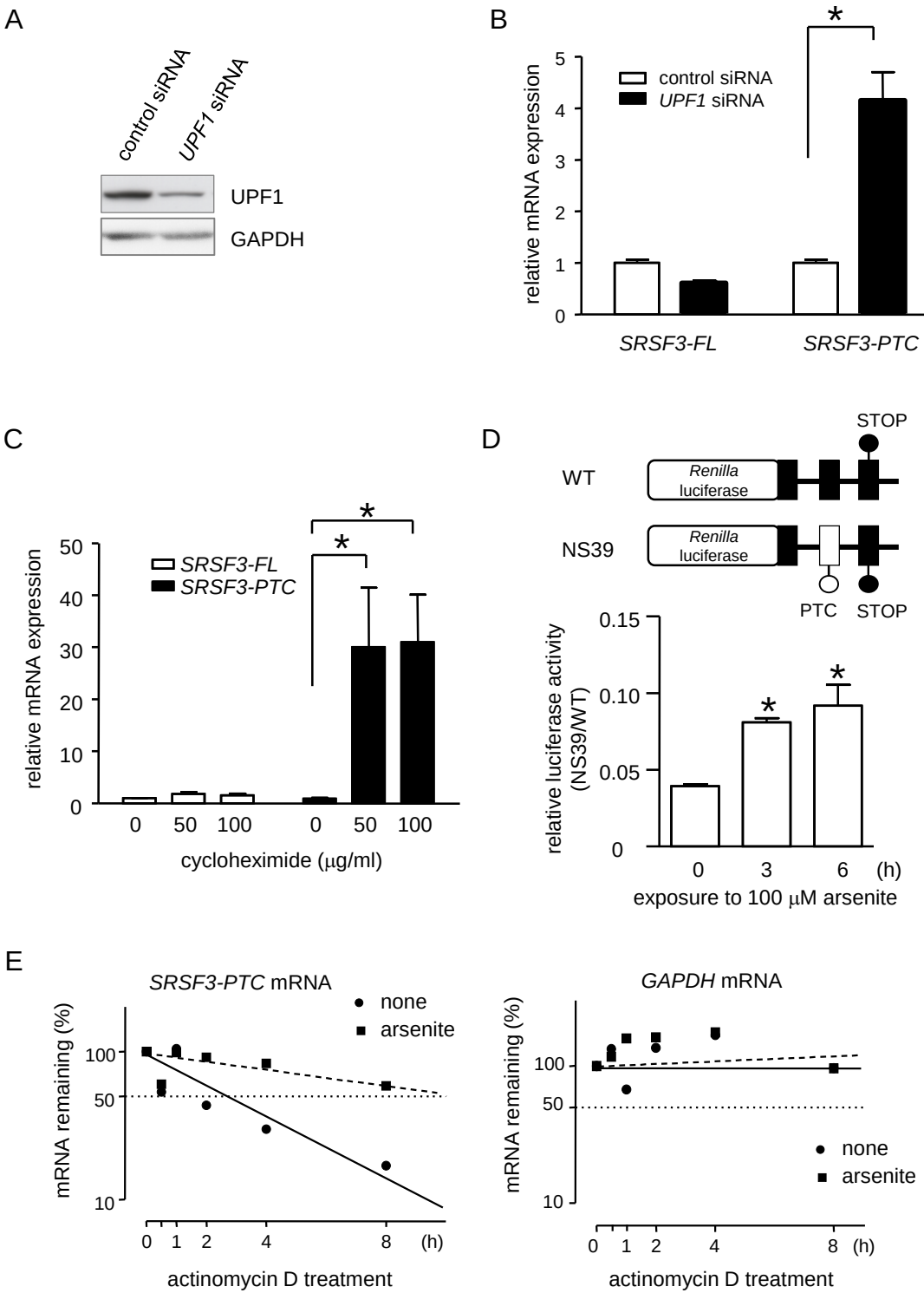
A
control siRNA
UPF1 siRNA
UPF1
GAPDH
B
control siRNA
UPF1 siRNA
relative mRNA expression
SRSF3-FL
SRSF3-PTC
C
SRSF3-FL
SRSF3-PTC
relative mRNA expression
cycloheximide (μg/ml)
D
STOP
WT
Renilla luciferase
NS39
PTC
STOP
relative luciferase activity (NS39/WT)
exposure to 100 μM arsenite
E
SRSF3-PTC mRNA
none
arsenite
mRNA remaining (%)
actinomycin D treatment
GAPDH mRNA
none
arsenite
mRNA remaining (%)
actinomycin D treatment

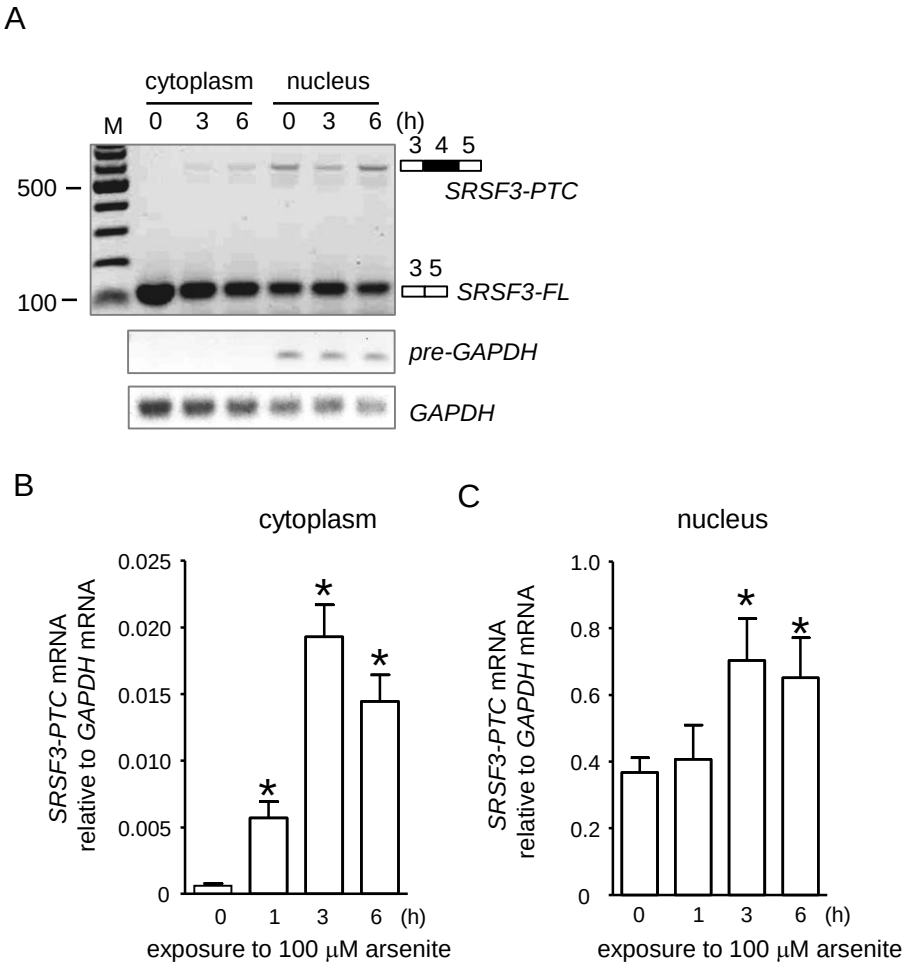
A
cytoplasm
nucleus
M
0 3 6 0 3 6 (h)
3 4 5
500
SRSF3-PTC
3 5
100
SRSF3-FL
pre-GAPDH
GAPDH
B
cytoplasm
SRSF3-PTC mRNA relative to GAPDH mRNA
0.025
0.020
0.015
0.010
0.005
0
0 1 3 6 (h)
exposure to 100 μM arsenite
C
nucleus
SRSF3-PTC mRNA relative to GAPDH mRNA
1.0
0.8
0.6
0.4
0.2
0
0 1 3 6 (h)
exposure to 100 μM arsenite

Fig. 5. *Kano et al.*

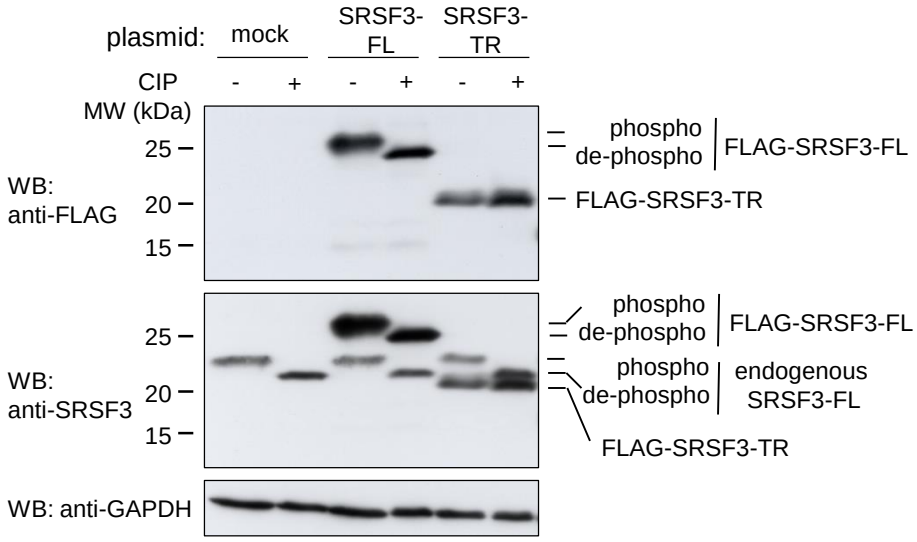

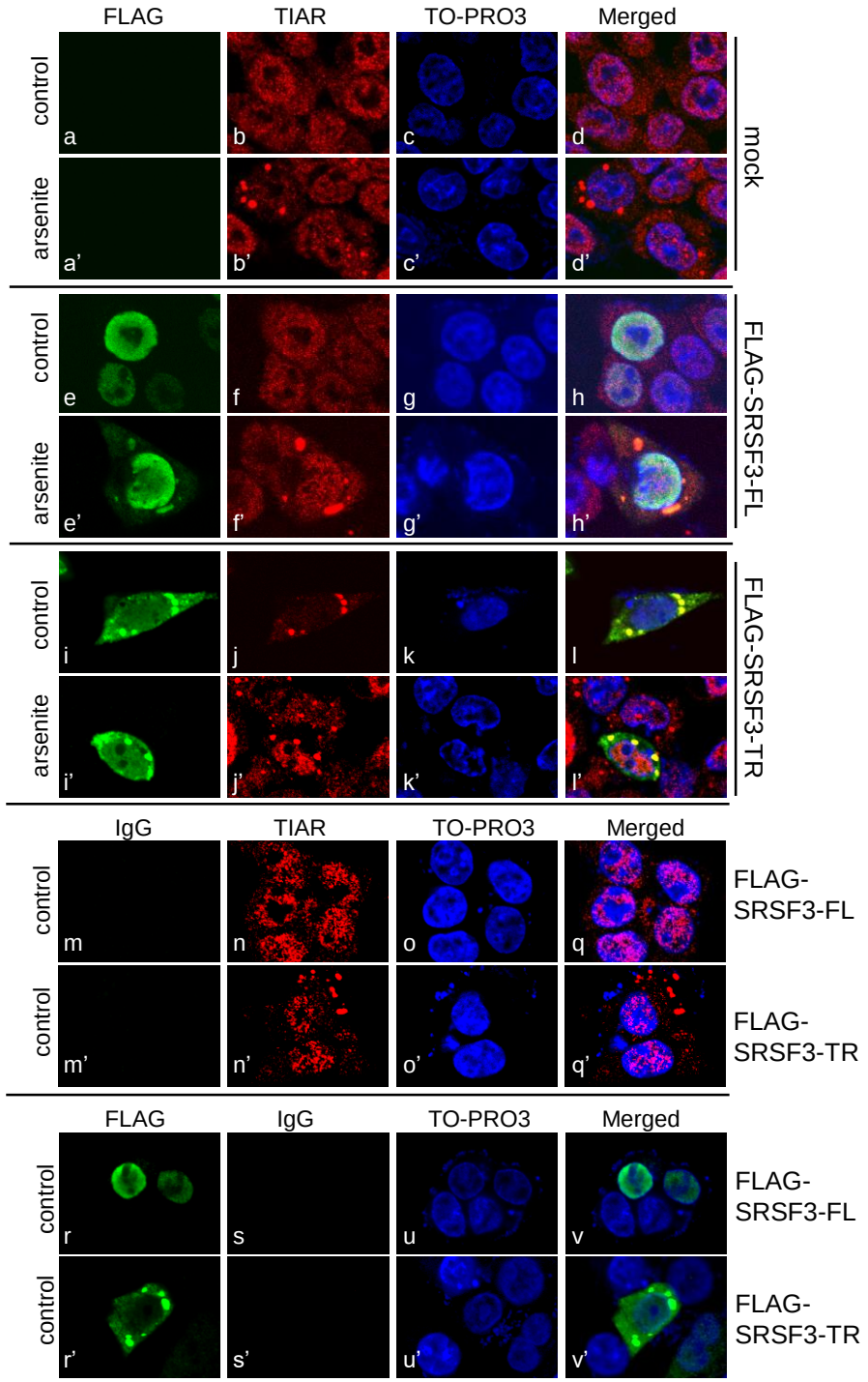
FLAG
TIAR
TO-PRO3
Merged
control
arsenite
a
b
c
d
a'
b'
c'
d'
mock
e
f
g
h
e'
f'
g'
h'
FLAG-SRSF3-FL
i
j
k
l
i'
j'
k'
l'
FLAG-SRSF3-TR
IgG
m
n
o
q
m'
n'
o'
q'
r
s
u
v
r'
s'
u'
v'

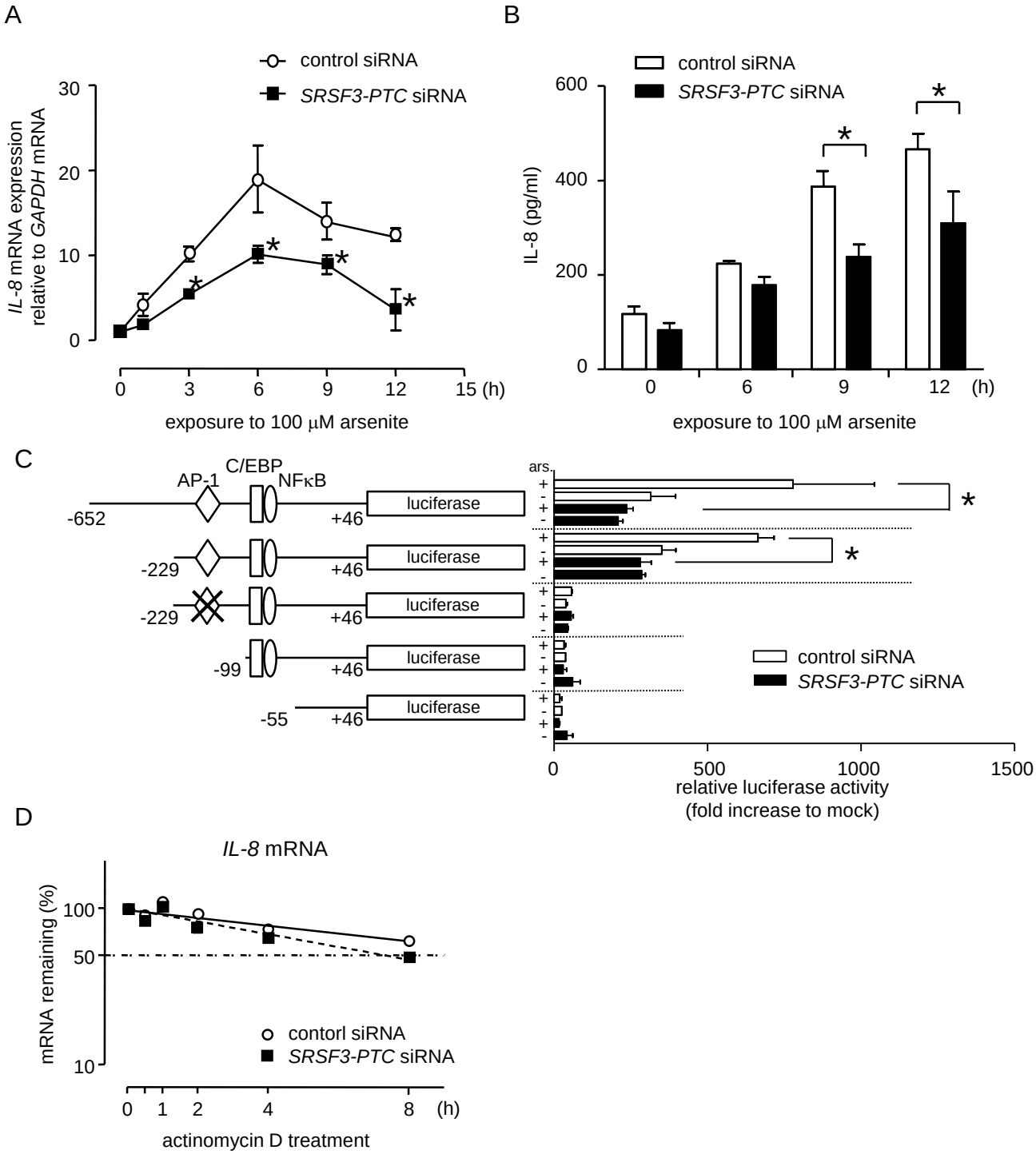
A
control siRNA
SRSF3-PTC siRNA
IL-8 mRNA expression relative to GAPDH mRNA
30
20
10
0
0
3
6
9
12
15 (h)
exposure to 100 μM arsenite
B
control siRNA
SRSF3-PTC siRNA
IL-8 (pg/ml)
600
400
200
0
0
6
9
12
(h)
exposure to 100 μM arsenite
C
AP-1
C/EBP
NFκB
-652
-229
-229
-99
-55
+46
luciferase
ars.
control siRNA
SRSF3-PTC siRNA
0
500
1000
1500
relative luciferase activity
(fold increase to mock)
D
IL-8 mRNA
mRNA remaining (%)
100
50
10
contorl siRNA
SRSF3-PTC siRNA
0
1
2
4
8
(h)
actinomycin D treatment

Fig. 8. *Kano et al.*

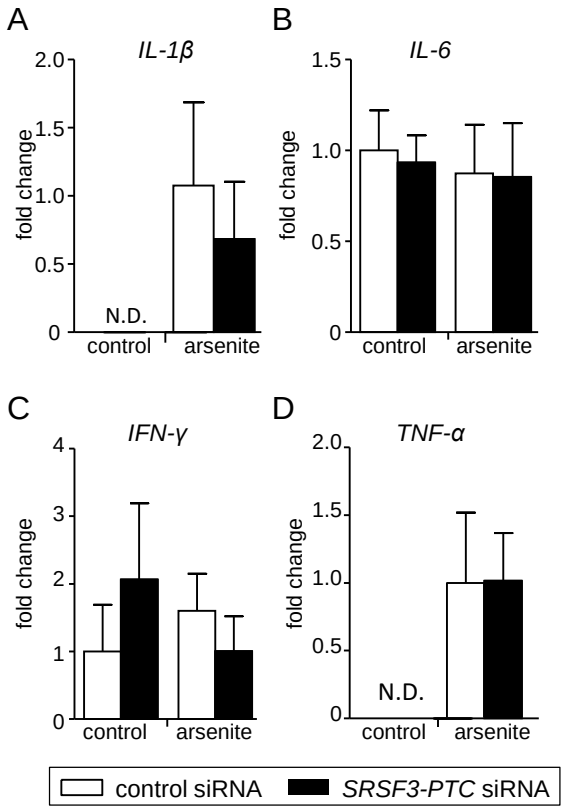

Fig. 9. *Kano et al.*

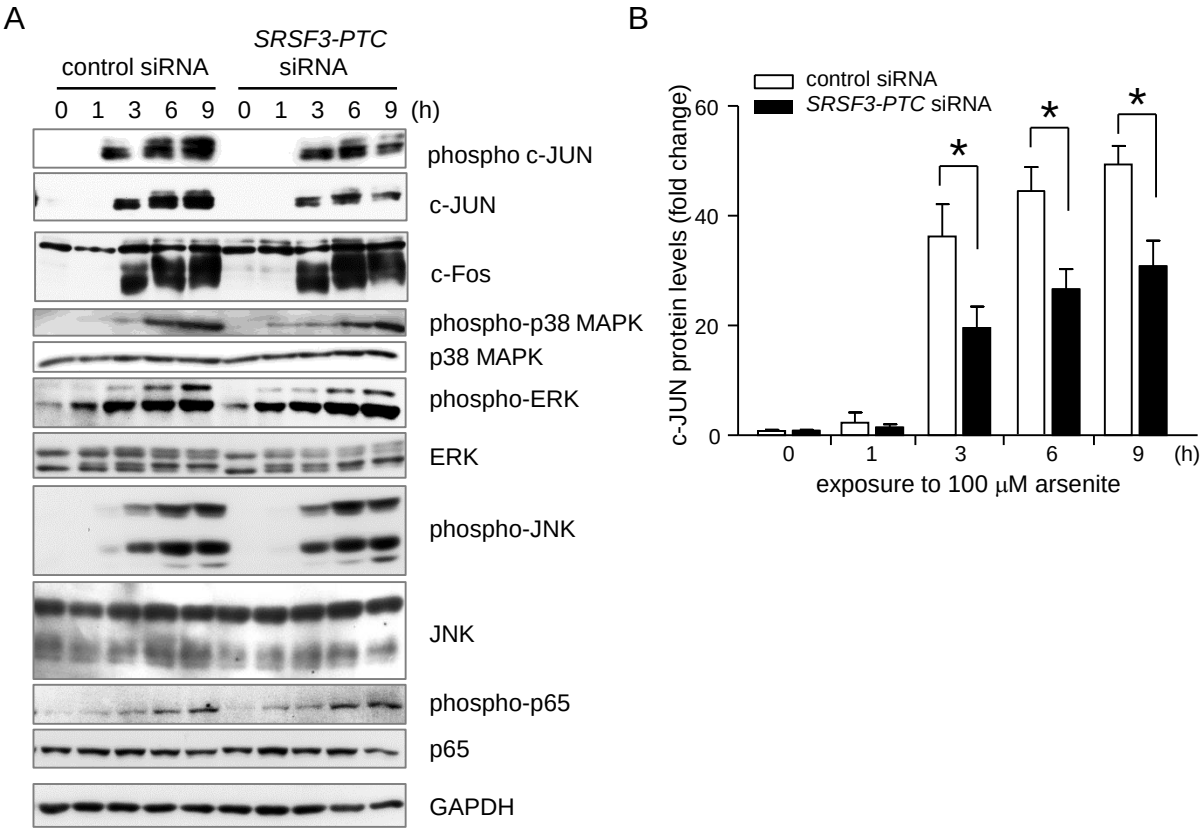

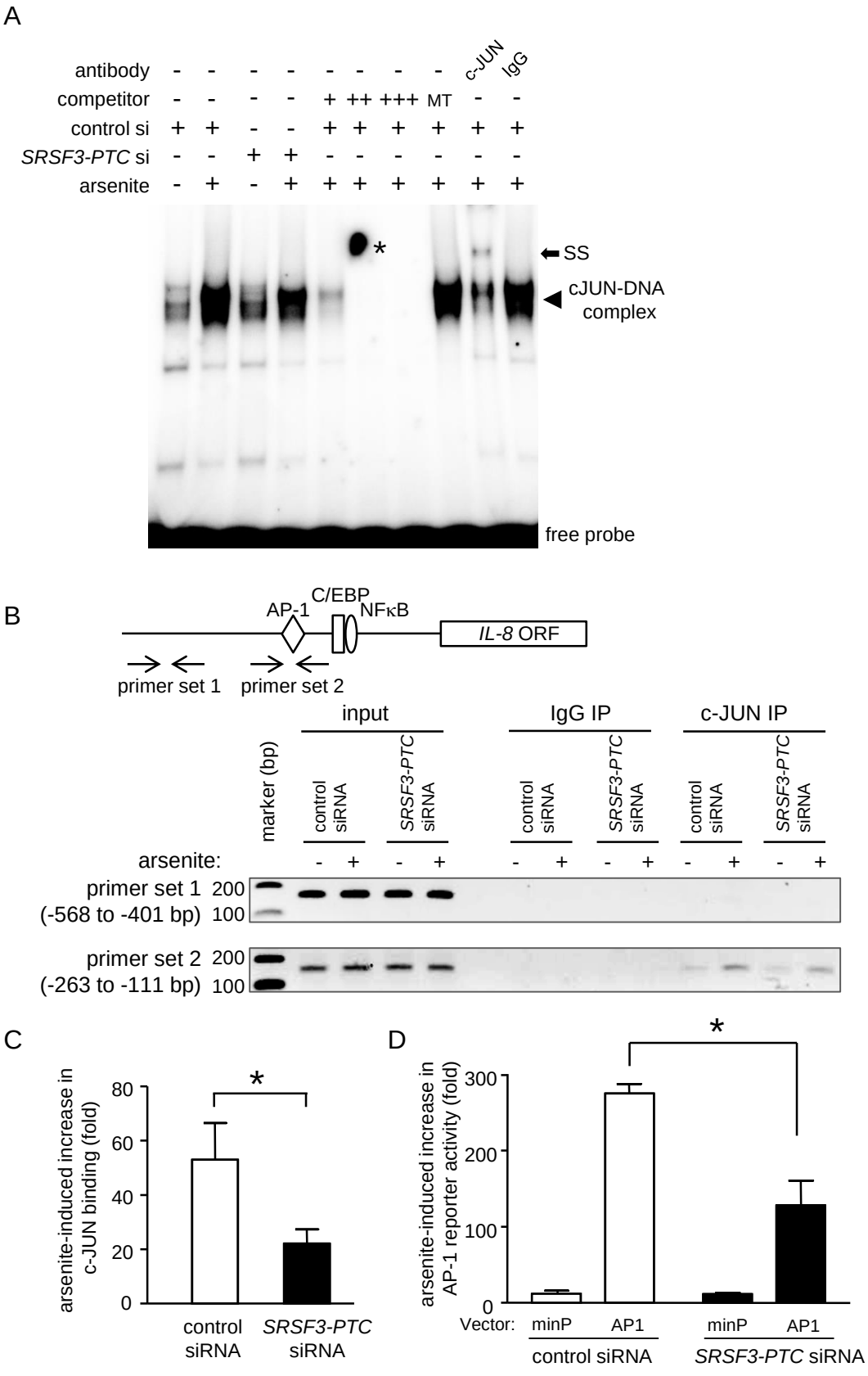
A
antibody - - - - - - - - c-JUN IgG
competitor - - - - + ++ +++ MT - -
control si + + - - + + + + + +
SRSF3-PTC si - - + + - - - - - -
arsenite - + - + + + + + + +
SS
cJUN-DNA complex
free probe
B
AP-1
C/EBP
NFκB
IL-8 ORF
primer set 1
primer set 2
input
IgG IP
c-JUN IP
marker (bp)
control siRNA
SRSF3-PTC siRNA
arsenite:
primer set 1 (-568 to -401 bp)
primer set 2 (-263 to -111 bp)
200
100
C
arsenite-induced increase in c-JUN binding (fold)
control siRNA
SRSF3-PTC siRNA
D
arsenite-induced increase in AP-1 reporter activity (fold)
Vector: minP AP1 minP AP1
control siRNA
SRSF3-PTC siRNA

Table 1. Primer sets used for reverse transcription (RT)-PCR and quantitative real-time RT-PCR (qPCR)

| Targets | | Primer Sequences (5' - 3') |
|---|---|---|
| *SRSF3-FL* | forward | GTGAAAAAAGAAGTAGAAATCGTGG |
| | reverse | CTCCTTCTTGGAGATCTGCGACGAG |
| *SRSF3-PTC* | forward | TCCACCTCGTCGCAGAGTCACCATC |
| | reverse | TCATGTGAAACGACACCAGCCAAGC |
| *GAPDH* | forward | AGCCACATCGCTCAGACAC |
| | reverse | GCCCAATACGACCAAATCC |
| *pre-GAPDH* | reverse | CCCATACGACTGCAAAGACC |
| *18S* | forward | CCCTATCAACTTTCGATGGTAGTCG |
| | reverse | CCAATGGATCCTCGTTAAAGGATTT |
| *IL-8* | forward | AGACAGCAGAGCACACAAGC |
| | reverse | AGGAAGGCTGCCAAGAGAG |
| *IL-1β* | forward | GGGCCTCAAGGAAAAGAATC |
| | reverse | TTCTGCTTGAGAGGTGCTGA |
| *IL-6* | forward | AGGAGACTTGCCTGGTGAAA |
| | reverse | CAGGGGTGGTTATTGCATCT |
| *IFN-γ* | forward | TCCCATGGGTTGTGTGTTTA |
| | reverse | AAGCACCAGGCATGAAATCT |
| *TNF-α* | forward | TCCTTCAGACACCCTCAACC |
| | reverse | AGGCCCCAGTTTGAATTCTT |